

# arxiv一周文献泛读200817-200821

## 200817

### [IceCube Search for High-Energy Neutrino Emission from TeV Pulsar Wind Nebulae](#)

<https://arxiv.org/abs/2003.12071>

type:observation-neutrino&pulsar\_wind\_nebulae

comment:本文使用IceCube9.5年的全天数据，报告了对辐射高能伽马射线的35个PWNe进行中微子辐射搜寻的stacking分析结果,没有发现明显关联.

► details

Authors: M. G. Aartsen, M. Ackermann, J. Adams, et al.

Comments: 11 pages, 2 figures; matches the published version in ApJ

Pulsar wind nebulae (PWNe) are the main gamma-ray emitters in the Galactic plane. They are diffuse nebulae that emit nonthermal radiation. Pulsar winds, relativistic magnetized outflows from the central star, shocked in the ambient medium produce a multiwavelength emission from the radio through gamma rays. Although the leptonic scenario is able to explain most PWNe emission, a hadronic contribution cannot be excluded. A possible hadronic contribution to the high-energy gamma-ray emission inevitably leads to the production of neutrinos. Using 9.5 yr of all-sky IceCube data, we report results from a stacking analysis to search for neutrino emission from 35 PWNe that are high-energy gamma-ray emitters. In the absence of any significant correlation, we set upper limits on the total neutrino emission from those PWNe and constraints on hadronic spectral components.

- 脉冲星风星云PWNe是具有非热辐射的弥散星云，脉冲星风是来自中心源的相对论性磁化外流，与周围介质相互作用而产生从射电到伽马射线的多波段辐射。
- 脉冲星风星云是银道面上主要的gamma-ray辐射源。
- 尽管轻子情形可以解释大部分PWNe辐射，也不能否定存在来自重子的贡献。如果在高能伽马射线辐射中存在重子的贡献，就不可避免会产生中微子。
- 本文使用IceCube9.5年的全天数据，报告了对辐射高能伽马射线的35个PWNe进行中微子辐射搜寻的stacking分析结果。
- 在没有发现明显的关联的结果下，作者给出了这些PWNe的总中微子辐射的上限，对重子光谱成分进行了限制。

# The Carnegie Supernova Project-I: Correlation Between Type Ia Supernovae and Their Host Galaxies from Optical to Near-Infrared Bands

<https://arxiv.org/abs/2006.15164>

type:observation-laSN

comment:报道了Carnegie Supernova Project-I (CSP-I)项目中观测的Ia型SN的宿主星系的光学近红外测光

► details

Authors: Syed A. Uddin, Christopher R. Burns, M. M. Phillips et al.

Comments: Accepted to The Astrophysical Journal

We present optical and near-infrared ( $ugriYJH$ ) photometry of host galaxies of Type Ia supernovae (SN Ia) observed by the Carnegie Supernova Project-I. We determine host galaxy stellar masses and, for the first time, study their correlation with SN Ia **standardized** luminosity across optical and near-infrared ( $uBgVriYJH$ ) bands. In the individual bands, we find that SNe Ia are more luminous in more massive hosts with **luminosity offsets** ranging between  $-0.07 \pm 0.03$  mag to  $-0.15 \pm 0.04$  mag after **light-curve standardization**. The slope of the SN Ia Hubble residual-host mass relation is negative across all  $uBgVriYJH$  bands with values ranging between  $-0.036 \pm 0.025$  mag/dex to  $-0.097 \pm 0.027$  mag/dex -- implying that **SNe Ia in more massive galaxies are brighter than expected**. The near-constant observed correlations across optical and near-infrared bands indicate that dust may not play a significant role in the observed **luminosity offset**--host mass correlation. We measure projected separations between SNe Ia and their host centers, and find that SNe Ia that explode beyond a projected 10 kpc have a 30% to 50% reduction of the dispersion in Hubble residuals across all bands -- making them a more uniform subset of SNe~Ia. Dust in host galaxies, peculiar velocities of nearby SN Ia, or a combination of both may drive this result as the **color excesses** of SNe Ia beyond 10 kpc are found to be generally lower than those interior, but there is also a diminishing trend of the dispersion as we exclude nearby events. We do not find that SN Ia average luminosity varies significantly when they are grouped in various **host morphological types**. Host galaxy data from this work will be useful, in conjunction with future high-redshift samples, in constraining cosmological parameters.

- 作者报道了Carnegie Supernova Project-I (CSP-I)项目中观测的Ia型SN的宿主星系的光学近红外测光。
  - CSP-I 2004-2010, 主要对低红移 ( $0 < z < 0.1$ ) 的SNe 进行精准的多波段光变曲线测光观测以及光谱的获取。
- 决定了宿主星系质量, 首次研究了它们与Ia型SN从光学到近红外 ( $uBgVriYJH$ ) 波段标准化光度间的关系。

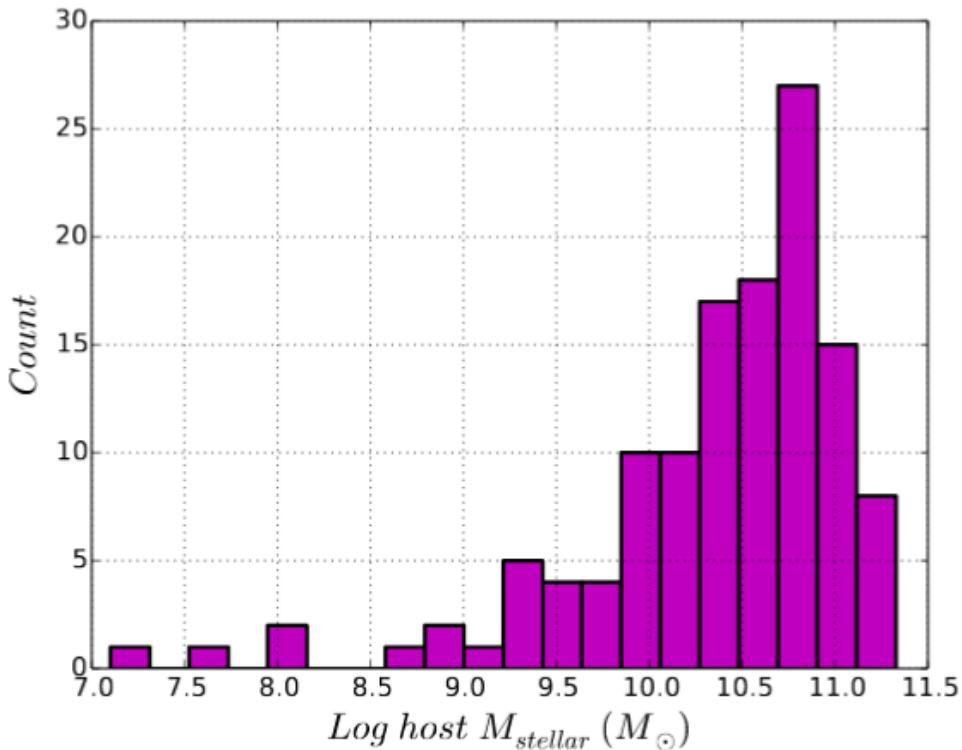


**Figure 3.** Distribution of host galaxy stellar mass of SNe Ia from CSP-I. The distribution has a peak at a relatively higher mass, which is a consequence of galaxy-targeted SN Ia searches.

- 在单个波段，发现更大质量星系的Ia型SN会更明亮，with **luminosity offsets** ranging between  $-0.07 \pm 0.03$  mag to  $-0.15 \pm 0.04$  mag after **light-curve standardization**(correcting for the luminosity-decline rate relation).
- Ia型 SN 哈勃残差-宿主星系质量的相关性在所有  $uBgVriYJH$  波段都是负值，变化范围为  $-0.029 \pm 0.029$  mag/dex to  $-0.093 \pm 0.031$  mag/dex，这表明更大质量星系的Ia型SN比预期的更亮（由于斜率是负数，质量越大即哈勃残差绝对值越大，即实际越亮）。
  - The Hubble residual is the deviation of the inferred distance modulus to the SN, calculated from its apparent luminosity and light curve properties, away from the expected value at the SN redshift. [Kelly et al 2009](#)
  - Hubble residual is the difference between the predicted and the observed values of distance moduli after obtaining a best-fit cosmological model for a given set of SNe Ia. We will refer to Hubble residuals as luminosities in such a way that negative values indicate more luminous SNe Ia. This work

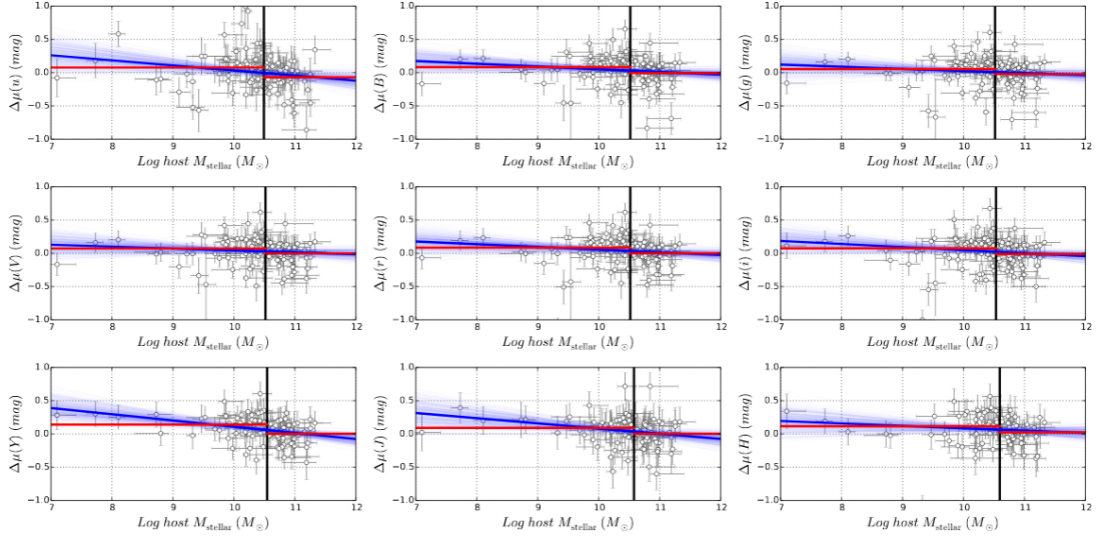


**Figure 7.** SN Ia Hubble residual ( $\Delta\mu$ ) vs host stellar mass across  $uBgVriYJH$  bands. In each case, the vertical solid black line shows the median split point, the slanted blue thick solid line shows the best-fit linear trend with lighter blue lines contain the 95% pointwise confidence intervals on the regression line, and red solid lines show the weighted mean of Hubble residuals at both sides of the split point. Slopes of the best-fit lines and Hubble residual offsets are presented in Table 2.

- 从光学到近红外波段上观测的相关性近似不变，表明尘埃在观测到的**luminosity offset--host mass correlation**中没有显著影响。
- 测量了Ia型SNe 距离它们宿主星系中心的投影距离，发现在10kpc以上爆发的Ia SN的各波段哈勃残差的弥散要小30%到50%，表明这部分SN是一个更均匀的Ia SN 的子集。宿主星系的尘埃，邻近Ia SN的peculiar velocity (refers to the motion of an object relative to a Galactic rest fram)，都可能导致这样的结果。

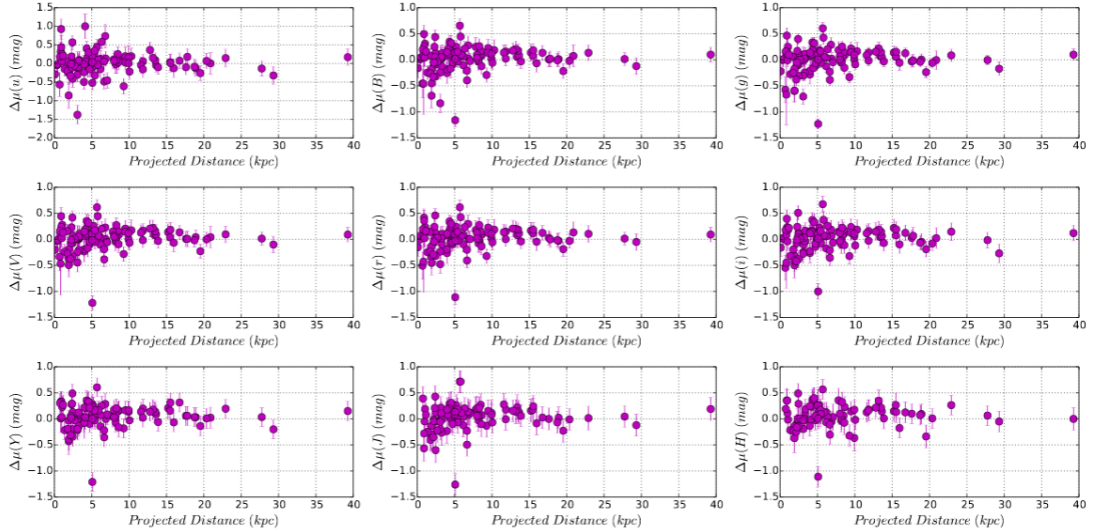


**Figure 14.** Variation of  $\Delta\mu$  with projected distance from host centers in  $uBgVriYJH$  bands. In all cases  $\Delta\mu$  have smaller dispersion when they explode farther from their host centers.

- 另外，10kpc以上 Ia SNe 的 color excesses 普遍低于10kpc以内的，but there is also a diminishing trend of the dispersion as we exclude nearby events.

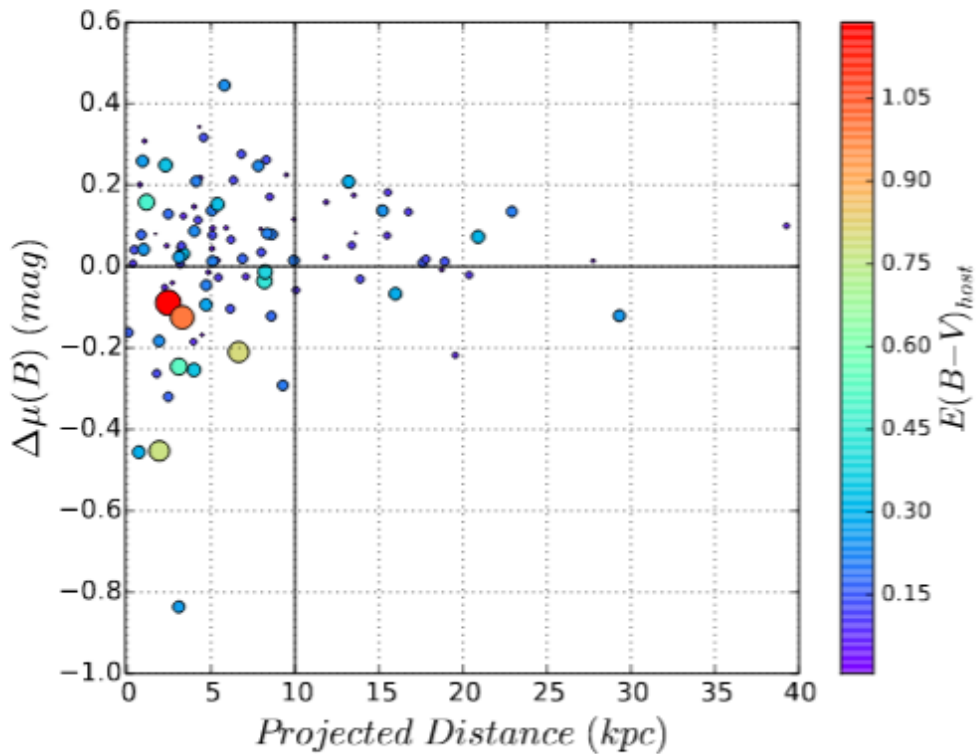


**Figure 15.** Plot of SN Ia  $B$ -band Hubble residual vs. projected distances from host centers. Symbols in this dispersion plot are varying according to respective color excess values,  $E(B - V)_{\text{host}}$ . Redder and larger symbols refer to higher color excess. SNe Ia with larger color excess tend to reside closer to hosts and are more luminous.

- 如果按照宿主形态类型把Ia SNe 进行分组，没有发现 Ia SNe 平均光度有显著的变化。

## 200818

### Analytic solutions for neutrino-light curves of core-collapse supernovae

<https://arxiv.org/abs/2008.07070>

type:theory-SN

comment:提出了一个核塌缩超新星的中微子辐射光变曲线的解析模型

► details

Athours: Yudai Suwa (Kyoto Sangyo U. & YITP), Akira Harada (ICRR), Ken'ichiro Nakazato (Kyushu U.), Kohsuke Sumiyoshi (NIT, Numazu College)

Comments: 12 pages, 1 figure, 1 table

Neutrino is a guaranteed signal from supernova explosions in the Milky Way and is the most valuable messenger that can provide us with information about the deepest part of supernovae. In particular, neutrinos will provide us with physical quantities, such as the radius and mass of protoneutron stars (PNS), which are the central engine of supernovae. It requires a theoretical model that connects observables such as neutrino luminosity and average energy with physical quantities. Here we show analytic solutions for the neutrino-light curve derived from the neutrino radiation transport equation by employing the diffusion approximation and the analytic density solution of the hydrostatic equation for the PNS. The neutrino luminosity and the average energy as functions of time are explicitly presented, with dependence on PNS mass, radius, the total energy of neutrinos, surface density, and opacity. The analytic solutions provide good representations of the numerical models from a few seconds after the explosion and let our rough estimate of these physical quantities to be made from observational data.

- 文章提出了一个核塌缩超新星的中微子辐射光变曲线的解析模型。如中微子光度和平均能量随时间的变化关系，其中涉及到PNS(prototypeneutron star)质量，半径，中微子总能亮，表面密度，不透明度等参数。
- 此模型可描述爆后 $\sim 1$ s的中微子辐射行为。

The corresponding neutrino luminosity is given as

$$L = 3.3 \times 10^{51} \text{ erg s}^{-1} \left( \frac{M_{\text{PNS}}}{1.4M_{\odot}} \right)^6 \left( \frac{R_{\text{PNS}}}{10 \text{ km}} \right)^{-6} \left( \frac{g\beta}{3} \right)^4 \left( \frac{t + t_0}{100 \text{ s}} \right)^{-6}. \quad (47)$$

Integrating  $L$  over time and giving the total energy emitted by neutrinos  $E_{\text{tot}}$ ,  $t_0$  is given by

$$t_0 = 210 \text{ s} \left( \frac{M_{\text{PNS}}}{1.4M_{\odot}} \right)^{6/5} \left( \frac{R_{\text{PNS}}}{10 \text{ km}} \right)^{-6/5} \left( \frac{g\beta}{3} \right)^{4/5} \left( \frac{E_{\text{tot}}}{10^{52} \text{ erg}} \right)^{-1/5}. \quad (48)$$

The average energy of neutrinos is given by

$$\langle E_{\nu} \rangle := \frac{F_3}{F_2} k_B T(\xi_{\nu}) = 16 \text{ MeV} \left( \frac{M_{\text{PNS}}}{1.4M_{\odot}} \right)^{3/2} \left( \frac{R_{\text{PNS}}}{10 \text{ km}} \right)^{-2} \left( \frac{g\beta}{3} \right) \left( \frac{t + t_0}{100 \text{ s}} \right)^{-3/2}. \quad (49)$$

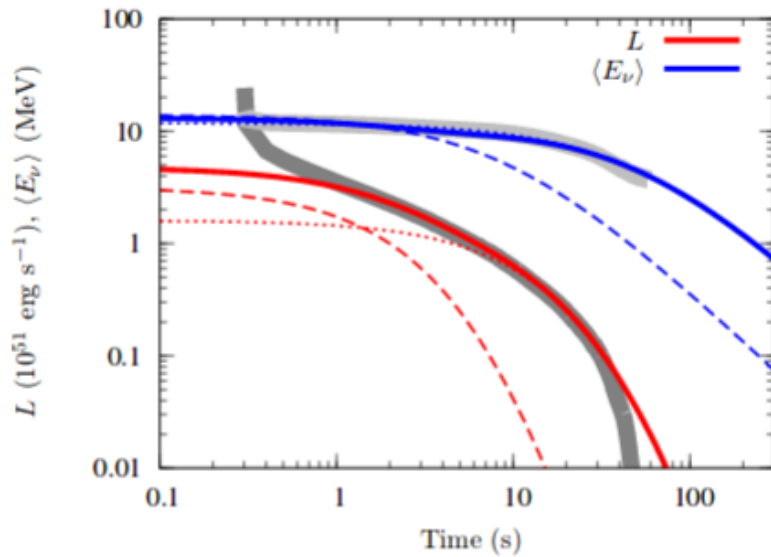


**Fig. 1** Luminosity (red) and average energy (blue) evolution for a flavor of neutrinos. The first component is a model with  $\beta = 3$  and  $E_{\text{tot}} = 4 \times 10^{52}$  erg and the second component is a model with  $\beta = 40$  and  $E_{\text{tot}} = 1 \times 10^{53}$  erg. For both components,  $M_{\text{PNS}} = 1.5M_{\odot}$ ,  $R_{\text{PNS}} = 12 \text{ km}$ , and  $g = 0.04$ . Grey lines are luminosity and average energy of  $\bar{\nu}_e$  of the model 147S in Ref. [12].

# The early discovery of SN 2017ahn: signatures of persistent interaction in a fast declining Type II supernova

<https://arxiv.org/abs/2008.06515>

type:observation-II SN

comment:报道了对一颗邻近Type II SN 2017ahn的长期跟踪观测。从爆后1天内到星云阶段，一共约470天

► details

Authors: L. Tartaglia, D. J. Sand, J. H. Groh et al.

Comments: 24 pages (20+Appendices), 16 figures, 4 tables, submitted to ApJ

We present high-cadence, comprehensive data on the nearby ( $D \approx 33\text{Mpc}$ ) Type II SN 2017ahn, discovered within  $\sim 1$  day of explosion, from the very early phases after explosion to the nebular phase. The observables of SN 2017ahn show a significant evolution over the  $\approx 470\text{d}$  of our follow-up campaign, first showing prominent, narrow Balmer lines and other high-ionization features purely in emission (i.e. flash spectroscopy features), which progressively fade and lead to a spectroscopic evolution similar to that of more canonical Type II supernovae. Over the same period, the decline of the light curves in all bands is fast, resembling the photometric evolution of linearly declining H-rich core-collapse supernovae. The modeling of the light curves and early flash spectra suggest a complex circumstellar medium surrounding the progenitor star at the time of explosion, with a first dense shell produced during the very late stages of its evolution being swept up by the rapidly expanding ejecta within the first  $\sim 6\text{d}$  of the supernova evolution, while signatures of interaction are observed also at later phases. Hydrodynamical models support the scenario in which linearly declining Type II supernovae are predicted to arise from massive yellow super/hyper giants depleted of most of their hydrogen layers.

- 报道了对一颗邻近Type II SN 2017ahn的长期跟踪观测。从爆后1天内到星云阶段，一共约470天。
  - 2017 02 8.29 由Cerro Tololo Inter-American Observatory (CTIO,Cerro Pachón, Chile).的0.41米 PROMPT5望远镜发现。
  - 后续观测大多使用了Las Cumbres Observatory network (Brown et al. 2013) within the Supernova Key Project的仪器，部分数据使用了挂载于智利ESO La Silla Observatory 2.2米的MPG望远镜上的Gamma-Ray Burst Optical/Near-Infrared Detector (GROND)
- 观测上表现出明显的演化行为，首先是有显著的窄Balmer线系以及其它的高电离度的发射特征（如耀发光谱特征），约一周后逐渐衰减并与大多数典型II型超新星的光谱演化相似。
- 在同一阶段，所有波段的光变曲线的衰减都很快，与线性衰减的H-rich核塌缩超新星的光变相似。

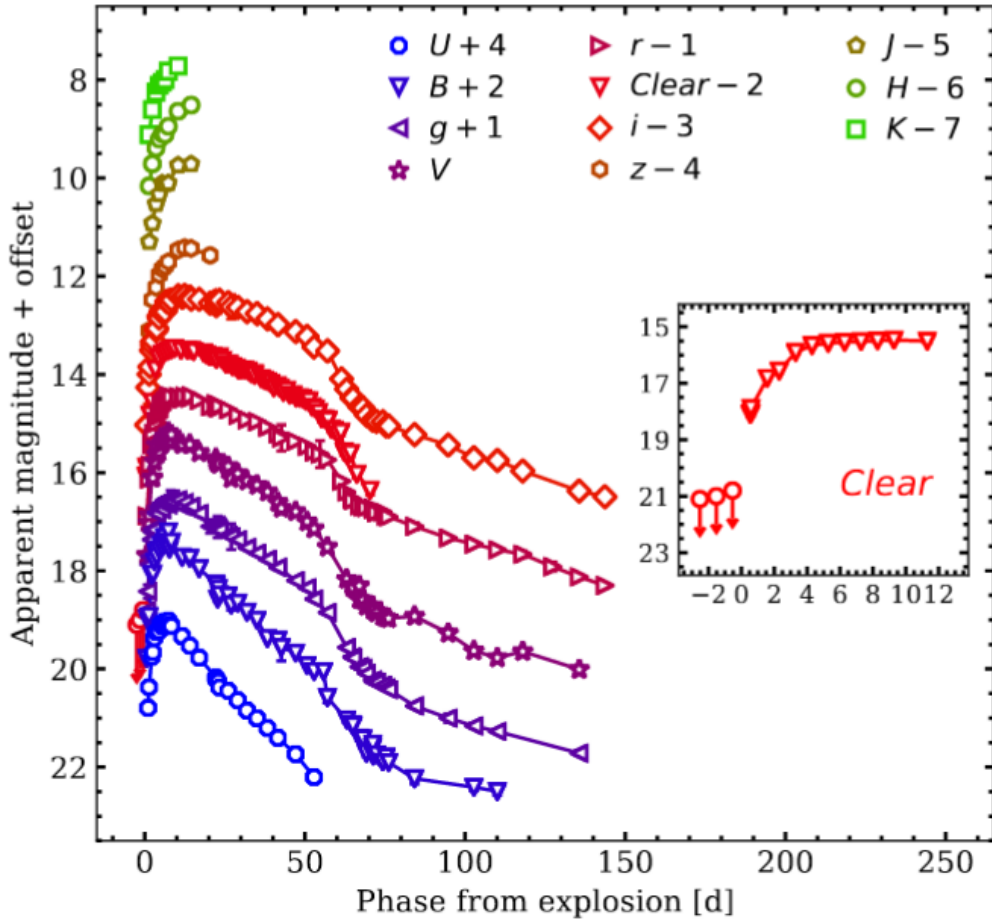


**Figure 2.** Optical and NIR light curves of SN 2017ahn.  $U, B, V, Clear, J, H, K$  and  $g, r, i, z$  magnitudes were calibrated to the Vega and AB photometric systems, respectively. Magnitudes were not corrected for the foreground Galactic or host extinction. Phases refer to the estimated epoch of the explosion. In the inset a zoom-in shows the last non-detection limits and the early evolution of the DLT40 data.

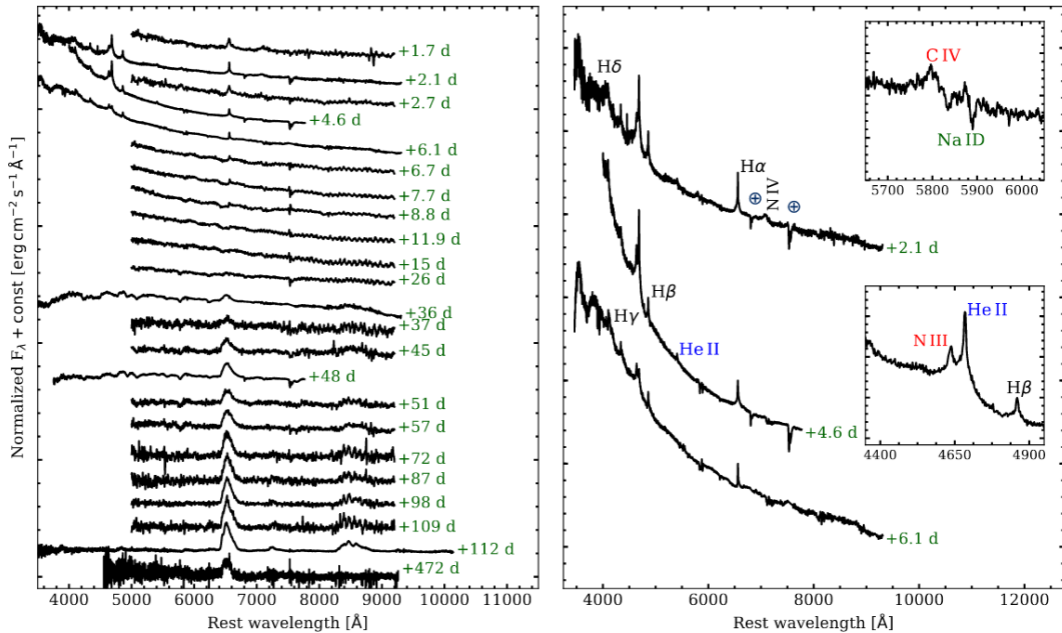


**Figure 6.** **Left:** Optical spectra of SN 2017ahn. Spectra were corrected for the total reddening along the line of sight. **Right:** Early evolution including higher resolution and signal-to-noise spectra. The most prominent features are identified.  $\oplus$  symbols mark the position of the main telluric absorption features. Insets show zoom-in regions around Na ID (**upper** inset, including C IV  $\lambda 5801$  at +2.1 d) and He II  $\lambda 4686$  (**bottom** panel, including C III/C IV  $\lambda 4650$ ) at +4.6 d.

- 对光变曲线和早期耀发光谱的模型拟合表明爆发时前身星周围的介质比较复杂，在约6天内，密度大的壳层被后面迅速扩张的抛射物扫过（with a first dense shell produced during the very late stages of its evolution being swept up by the rapidly expanding ejecta within the first  $\sim 6$ d of the supernova evolution），同时在晚期也观测到了相互作用的迹象。
- 流体动力学模型支持线性衰减的II型超新星来自于耗尽大部分氢层的yellow super/hyper giants。

## Repeating behaviour of FRB 121102: periodicity, waiting times and energy distribution

<https://arxiv.org/abs/2008.03461>

type:observation-FRB

comment:讨论了FRB 121102 的周期性，爆发时间间隔和能量分布的情况,发现强簇集性的确是周期活动的结果，而且如果忽略少量毫秒级别的时间间隔，样本就呈现一个泊松分布

► details

Authors: M. Cruces, L. G. Spitler, P. Scholz et al.

Since the discovery of repetition it has been clear that the detections of fast radio burst (FRB) 121102 are **clustered**. Recently, it was argued that it is periodic, raising the question of whether the clustering reflected a not-yet-defined periodicity. We performed an extensive multi-wavelength campaign with Effelsberg, Green Bank telescope and the Arecibo observatory to **shadow** the Gran Telescopio Canaria (optical), NuSTAR (X-ray) and INTEGRAL (gamma-ray). We detected 36 bursts with Effelsberg, one with a pulse width of 39ms. **We tested the periodicity hypothesis using 165-hr of Effelsberg, and find a periodicity of  $161 \pm 5$  days.** We predict the source to be active from 2020-07-09 to 2020-10-

14 and, posteriorly, from 2020-12-17 to 2021-03-24. With the bursts detected, we compare the **waiting times** between consecutive bursts with a Weibull distribution with shape parameter  $k < 1$ , and a Poissonian distribution. We conclude that the strong clustering was indeed a consequence of a periodic activity and show that if few events of millisecond scale separation are excluded, the sample agrees with a Poissonian distribution. We model the bursts cumulative energy distribution, with energies from  $\sim 10^{38} - 10^{39}$  erg, and find that it is well described by a power-law with slope of  $\gamma = -1.1 \pm 0.2$ . We exclude a time changing slope to reconcile the discrepancies between the published values and propose that a single power-law might not fit the data over many orders of magnitude. With one burst detected during simultaneous NuSTAR observations, we place a  $5\sigma$  upper limit of  $6 - 40 \times 10^{46}$  erg on the 3–79 keV energy of an X-ray burst counterpart.

- 本文讨论了FRB 121102 的周期性，爆发时间间隔和能量分布的情况。
- 对于FRB 121102的探测是簇集的（clustered）。这些簇集的爆发是否反映了还未被定义的周期性？
- 作者利用Effelsberg（17年9月到20年6月）、Green Bank和Arecibo进行了长期的多波段观测to **shadow** the Gran Telescopio Canaria (optical), NuSTAR (X-ray) and INTEGRAL (gamma-ray)。
- Effelsberg探测到了36个爆，其中一个的脉冲宽度为39ms。作者对165小时的Effelsberg观测数据进行了周期性检验，发现 $161 \pm 5$ 天的周期性行为，预测此源在2020-07-09 to 2020-10-14为活跃期，下一个活跃期为2020-12-17 to 2021-03-24。
- 作者把这些连续探测间等待时间与形状参数 $k < 1$ 的韦伯分布以及泊松分布比较，发现强簇集性的确是周期活动的结果，而且如果忽略少量毫秒级别的时间间隔，样本就呈现一个泊松分布。

**Table 5.** Posterior values for the event rate ( $r$ ) and shape parameter ( $k$ ) from a Weibull Statistics and the event rate  $r_p$  from a Poissonian distribution. Prime values indicate the outcome of excluding bursts with waiting times shorter than 1 second ( $\delta t < 1$  s). The event rates consider a fluence threshold 0.08 Jy ms for bursts with a 1 ms duration and S/N above 7, and the confidence intervals shown assume  $1\sigma$  uncertainties.

Dataset	$r_p$ (day $^{-1}$ )	$r$ (day $^{-1}$ )	$k$	$r'_p$ (day $^{-1}$ )	$r'$ (day $^{-1}$ )	$k'$
All	$8 \pm 3$	$7_{-2}^{+3}$	$0.40_{-0.03}^{+0.04}$	$8 \pm 3$	$7_{-2}^{+3}$	$0.43_{-0.03}^{+0.04}$
On- $\phi$	$18 \pm 4$	$18_{-4}^{+5}$	$0.50_{-0.03}^{+0.05}$	$17 \pm 4$	$17_{-3}^{+5}$	$0.57_{-0.04}^{+0.06}$
November 2018	$82 \pm 9$	$76_{-21}^{+29}$	$0.6_{-0.1}^{+0.1}$	$79 \pm 9$	$76_{-19}^{+26}$	$0.7_{-0.1}^{+0.1}$
Gourdji et al. (2019)	$307 \pm 17$	$294_{-52}^{+57}$	$0.82_{-0.09}^{+0.1}$	$292 \pm 17$	$286_{-44}^{+44}$	$1.0_{-0.1}^{+0.2}$
Houben et al. (2019)	$20 \pm 4$	$18_{-5}^{+8}$	$1.0_{-0.2}^{+0.4}$	-	-	-

- 作者在拟合了 $\sim 10^{38} - 10^{39}$  erg能段的爆发累计能量分布，发现其较好符合斜率 $\gamma = -1.1 \pm 0.2$ 的幂率。
- 有一个爆同时被NuSTAR探测到，给出了X-射线对应体在3–79 keV 区间内的 $5\sigma$ 能量上限为 $6 - 40 \times 10^{46}$  erg

# SN2020bvc: a Broad-lined Type Ic Supernova with a Double-peaked Optical Light Curve and a Luminous X-ray and Radio Counterpart

<https://arxiv.org/abs/2004.10406>

type:observation-SN

comment:报道了对一个邻近宽线Ic型超新星 SN2020bvc的光学，射电和X射线观测。观测显示SN2020bvc与另一个Ic-BL SN2006aj有一些相似的性质，而后者与低光度GRB060218成协。

► details

Authors: Anna Y. Q. Ho, S. R. Kulkarni, Daniel A. Perley et al.

Comments: Accepted to ApJ. 39 pages, 17 figures. Comments welcome

We present optical, radio, and X-ray observations of SN2020bvc (=ASASSN20bs; ZTF20aalx1is), a nearby ( $z=0.0252$ ;  $d=114$  Mpc) broad-lined (BL) Type Ic supernova (SN). Our observations show that SN2020bvc shares several properties in common with the Ic-BL SN2006aj, which was associated with the low-luminosity gamma-ray burst (LLGRB) 060218. First, the 10 GHz radio light curve is on the faint end of LLGRB-SNe ( $L_{radio} \approx 10^{37} erg/s$ ): we model our VLA observations (spanning 13-43 d) as synchrotron emission from a mildly relativistic ( $v \gtrsim 0.3c$ ) forward shock. Second, with Swift and Chandra we detect X-ray emission ( $L_X \approx 10^{41} erg/s$ ) that is not naturally explained as inverse Compton emission or as part of the same synchrotron spectrum as the radio emission. Third, high-cadence (6×/night) data from the Zwicky Transient Facility (ZTF) shows a double-peaked optical light curve, the first peak from shock-cooling emission from extended low-mass material (mass  $M_e < 10^{-2} M_\odot$  at radius  $R > 10^{12} cm$ ) and the second peak from the radioactive decay of Ni-56. SN2020bvc is the first confirmed double-peaked Ic-BL SN discovered without a GRB trigger, so it is noteworthy that it shows X-ray and radio emission similar to LLGRB-SNe: this is consistent with models in which the same mechanism produces both the LLGRB and the shock-cooling emission. For four of the five other nearby ( $z \lesssim 0.05$ ) Ic-BL SNe with ZTF high-cadence data, we rule out a first peak like that seen in SN2006aj and SN2020bvc, i.e. that lasts  $\approx 1$  d and reaches a peak luminosity  $M \approx -18$ . X-ray and radio follow-up observations of future such events will establish whether double-peaked optical light curves are indeed predictive of LLGRB-like X-ray and radio emission.

- 报道了对一个邻近 ( $z=0.0252$ ;  $d=114$  Mpc) 的宽线Ic型超新星 SN2020bvc的光学，射电和X射线观测。观测显示SN2020bvc与另一个Ic-BL SN2006aj有一些相似的性质，而后者与低光度GRB060218成协。
  - 半数GRB-SNe成协的GRB是LLGRB,  $L_{\gamma,iso} < 10^{48.5} erg/s$ 。宇宙学GRB  $L_{\gamma,iso} > 10^{49.5} erg/s$ 。
  - LLGRB 的普遍程度是 宇宙学GRB的10倍到100倍 (Soderberg et al. 2006; Liang et al. 2007) , 但探测率很低, 样本很少, 传统GRBs, LLGRBs, Ic-BL SNe的联系还不清楚。
  - 通过光学-X射线-射电的观测来发现与GRB相关的但没有GRB触发的事件现象可以帮助加深对三者联系的理解。
  - SN2020bvc于2月4.34首次探测到 (P48) ,  $i = 17.48 \pm 0.05 mag$ ,  $ra = 14 : 33 : 57.01$ ,  $dec = 40 : 14 : 37.5$ 。而最近一次non-detection为ASAS-

SN的0.67天前即Feb 03.67,  $o > 19.4\text{mag}$ 。探测的2小时后P60的SEDM进行测谱, 光谱由热连续谱主导, 有一些宿主星系的氢线以及微弱的吸收线。在Feb 08.24使用Liverpool Telescope的SPRAT再次测谱, 显示出Ic-BL SN的特征。

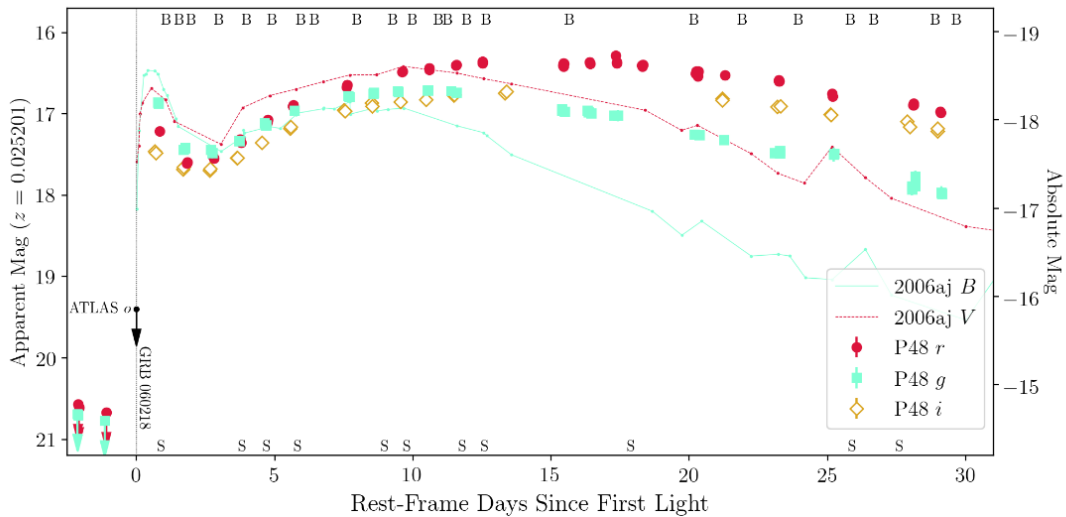


**Figure 2.**  $g$ -,  $r$ -, and  $i$ -band light curves of SN 2020bvc from the ZTF Uniform Depth Survey (ZUDS), and an upper limit from ATLAS. Measurements have been corrected for Milky Way extinction. Epochs of follow-up spectroscopy are indicated with an ‘S’ along the bottom of the figure. Epochs of blackbody fits (§3.2) are indicated with ‘B’ along the top of the figure. For comparison, we show  $B$  and  $V$ -band light curves of SN 2006aj ( $z = 0.033$ ) transformed to the redshift of SN 2020bvc ( $z = 0.025201$ ). The SN 2006aj light curve was taken from the Open Supernova Catalog and corrected for Milky Way extinction; the data is originally from Modjaz et al. (2006), Bianco et al. (2014), and Brown et al. (2014). We indicate the relative time of LLGRB 060218 compared to the light curve of SN 2006aj.

**Table 1.** Spectroscopic observations of SN 2020bvc. Epochs given since  $t_0$  as defined in §2.1. Velocities are derived from Fe II absorption features as described in §4.2.

Date (UTC)	$\Delta t$ (d)	Tel.+Instr.	Exp. Time (s)	$v_{\text{ph}}$ ( $10^4 \text{ km s}^{-1}$ )
Feb 04.43	0.76	P60+SEDM	1800	—
Feb 07.36	3.7	P60+SEDM	1800	$5.1 \pm 0.1$
Feb 08.24	4.6	LT+SPRAT	600	$2.58 \pm 0.51$
Feb 09.36	5.7	P60+SEDM	1800	—
Feb 12.51	8.8	P200+DBSP	600	$1.83 \pm 0.32$
Feb 13.33	9.7	P60+SEDM	1800	—
Feb 15.33	11.7	P60+SEDM	1800	—
Feb 16.14	12.5	NOT+ALFOSC	1200	$1.90 \pm 0.25$
Feb 21.43	17.7	P60+SEDM	1800	—
Feb 29.42	25.8	P60+SEDM	1800	—
Mar 02.14	27.5	NOT+ALFOSC	1200	—
Mar 17.19	42.6	LT+SPRAT	900	$1.72 \pm 0.32$
Mar 22.50	47.9	Keck1+LRIS	300	$1.79 \pm 0.39$

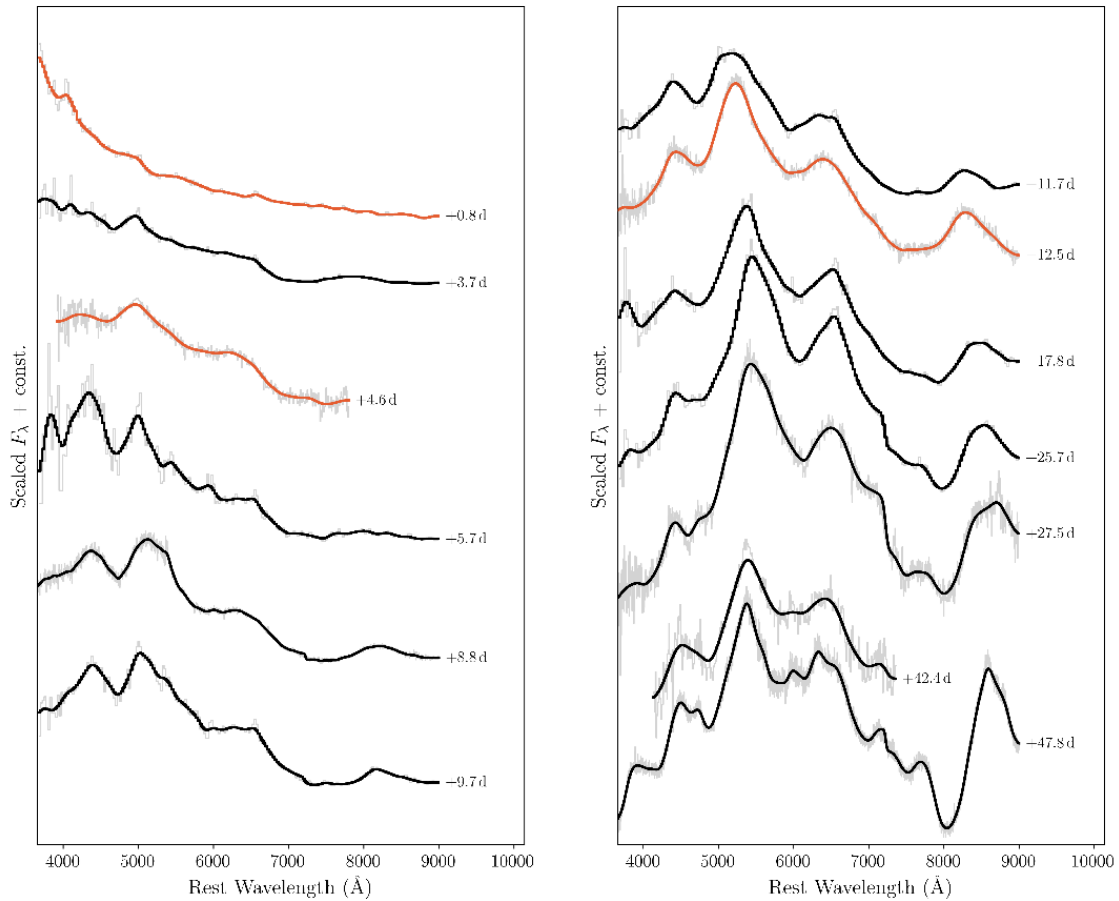


**Figure 4.** Optical spectra of SN 2020bvc. Phase is relative to  $t_0$ , defined in §2.1 as the time of last non-detection by ATLAS. The first spectrum is dominated by a blue continuum. By  $\Delta t = 5.7$  d the spectrum strongly resembled a Ic-BL SN. The raw spectrum is shown in light grey, and a smoothed spectrum (with host emission lines removed) is overlaid in black. Spectra highlighted in orange are plotted compared to LLGRB-SNe at similar phases in Figure 10.

- 首先，10GHz的射电光变曲线在LLGRB-SNe中处于弱端 ( $L_{radio} \approx 10^{37} erg/s$ )，采用来自轻相对论性前向激波 ( $v \geq 0.3c$ ) 的同步辐射情景来拟合VLA观测 (14-43d)。
- 其次，使用 $Swift$ 和 $Chandra$ 探测的X射线辐射 ( $L_X \approx 10^{41} erg/s$ ) 用逆康普顿散射或是用同步辐射都不能很好的解释观测 (that is **not naturally** explained as inverse Compton emission or as part of the same synchrotron spectrum as the radio emission.)，可能是多成分的辐射。
- 第三，高节奏 (6x/night) 的ZTF观测呈现了一个双峰的光变曲线，第一个峰来自延展的低质量物质 ( $mass M_e < 10^{-2} M_\odot$  at radius  $R > 10^{12} cm$ ) 的激波冷却 (shock-cooling)，第二个峰来自Ni-56的放射性衰变。
- SN2020bvc是第一个被证实的没有探测到GRB的双峰Ic-BL SN，而且它展示出了与LLGRB-SNe相似的X射线和射电辐射：这符合LLGRB和激波冷却辐射产生自相同机制的模型是符合的。
- 在另外5个ZTF观测的邻近 ( $z \leq 0.05$ ) 的Ic-BL SNe中，4个SN没有类似于SN2006aj和SN2020bvc第一个峰 (持续1天，峰值达到M=-18) 的峰。

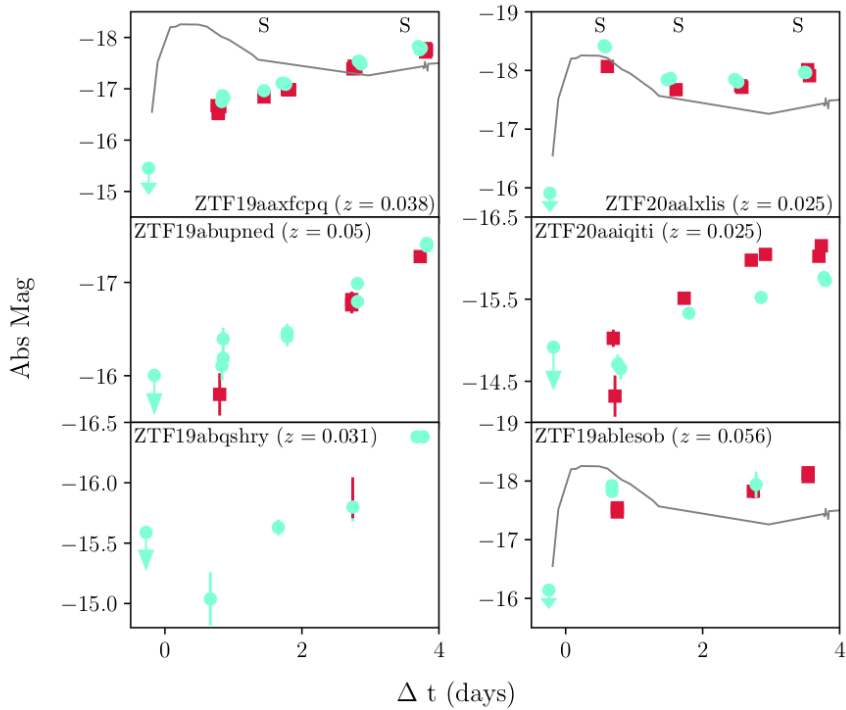


**Figure 17.** Early ( $\Delta t \lesssim 4$  d) light curves of nearby Ic-BL SNe observed as part of ZTF's high-cadence surveys, from forced photometry on P48 images (Yao et al. 2019). The  $B$ -band light curve of SN 2006aj is shown as a grey line for comparison. Epochs of follow-up spectroscopy are marked with 'S' along the top of the panel.

- 对未来这类事件的X射线和射电的跟踪观测将有助于确定双峰光学光变曲线是否能预测类LLGRB的X射线和射电辐射。

# Supernovae Ib and Ic from the explosion of helium stars

<https://arxiv.org/abs/2008.07601>

type:theory-ISN

comment:文章对相互作用双星中的氦星进行了演化模拟，用不同的参数（如 $^{56}\text{Ni}$ ，质量损失率，爆炸能量等）可以重现不同类型的Ib/Ic型SN的行为（如光变曲线，峰值光度等）

► details

Authors: Luc Dessart, Sung-Chul Yoon, David R. Aguilera-Dena, and Norbert Lange

Comments: Accepted for publication in A&A

Much difficulty has so far prevented the emergence of a consistent scenario for the origin of Type Ib and Ic supernovae (SNe). Either the SN rates, or the ejecta masses and composition were in tension with inferred properties from observations. Here, we follow a heuristic approach by examining the fate of helium stars in the mass range 4 to 12  $\text{M}_{\odot}$ , which presumably form in interacting binaries. The helium stars are evolved using stellar wind mass loss rates that agree with observations, and which reproduce the observed luminosity range of galactic WR stars, leading to stellar masses at core collapse in the range 3 to 5.5  $\text{M}_{\odot}$ . We then explode these models adopting an explosion energy proportional to the ejecta mass, roughly consistent with theoretical predictions. We impose a fixed  $^{56}\text{Ni}$  mass and strong mixing. The SN radiation from 3 to 100 d is computed self-consistently starting from the input stellar models using the time-dependent non-local thermodynamic equilibrium radiative-transfer code CMFGEN. By design, our fiducial models yield very similar light curves, with a rise time of about 20 d and a peak luminosity of  $\sim 10^{42.2} \text{ erg/s}$ , in line with representative SNe Ibc. **The less massive progenitors retain a He-rich envelope and reproduce the color, line widths, and line strengths of a representative sample of SNe Ib, while stellar winds remove most of the helium in the more massive progenitors, whose spectra match typical SNe Ic in detail.** The transition between the predicted Ib-like and Ic-like spectra is continuous, but it is sharp, such that the resulting models essentially form a dichotomy. Further models computed with varying explosion energy,  $^{56}\text{Ni}$  mass, and long-term power injection from the remnant show that a moderate variation of these parameters can reproduce much of the diversity of SNe Ibc. We conclude that stars stripped by a binary companion can account for the vast majority of ordinary Type Ib and Ic SNe, and that stellar wind mass loss is the key to remove the helium envelope in the progenitors of SNe Ic

- 文章对相互作用双星中的氦星进行了演化模拟，用不同的参数（如 $^{56}\text{Ni}$ ，质量损失率，爆炸能量等）可以重现不同类型的Ib/Ic型SN的行为（如光变曲线，峰值光度等）。
- 质量不那么大的前身星会保留富He的包层，可重现典型Ib型SN的颜色，线宽，线强度。
- 更大质量的前身星的氦被星风剥离，产生典型Ic型SN的光谱细节。
- 结论是在双星中被伴星剥离的恒星可以解释绝大多数的普通SNe-Ib和Ic，且星风质量损失是SN-Ic前身中氦包层被剥离的关键。

## Optical and spectral observations and hydrodynamic modelling of Type I Ib Supernova 2017gpn

<https://arxiv.org/abs/2008.07934>

type:observation-IIbSN

comment:对I Ib型超新星2017gpn进行了测光和测谱。这颗超新星是在LIGO/Virgo G299232引力波事件的误差天区中发现的

► details

Authors: Elena A. Balakina, Maria V. Pruzhinskaya, ... Xiaofeng Wang, Danfeng Xiang, Han Lin et al.

Comments: 18 pages, 13 figures

In this work we present the photometric and spectroscopic observations of Type I Ib Supernova 2017gpn. This supernova was discovered in the error-box of LIGO/Virgo G299232 gravitational-wave event. We obtained the light curves in B and R passbands and modelled them numerically using the one-dimensional radiation hydrocode STELLA. The best-fit model has the following parameters: the pre-SN star mass and the radius are 3.5 Msun and 50 Rsun, respectively; the explosion energy is  $E_{exp} = 1.2 * 10^{51} erg$ ; the mass of radioactive nickel is  $M_{56Ni} = 0.11M_{sun}$ , which is totally mixed through the ejecta, the mass of the hydrogen envelope 0.06 Msun. Moreover, SN 2017gpn is a confirmed SN I Ib that is located at the farthest distance from the center of its host galaxy NGC 1343 (i.e. the projected distance is about 21 kpc). This challenges the scenario of the origin of Type I Ib Supernovae from massive stars.

- 对I Ib型超新星2017gpn进行了测光和测谱。这颗超新星是在LIGO/Virgo G299232引力波事件的误差天区中发现的。
  - 在O2的最后一天2017 08 27.017，首先由MASTER发现，名为 MASTER OT J033744.97+723159.0
  - 作者使用SAO RAS 的 Zeiss-1000 望远镜进行了20次测光
  - 兴隆216参与了后续测谱，进一步证实SN类型
- 对B R波段的光变曲线进行了拟合 (one-dimensional radiation hydrocode STELLA) ，最佳拟合参数为：
  - 前身星质量和半径： $3.5 M_{\odot}$ ， $50 R_{\odot}$
  - 爆炸能量： $E_{exp} = 1.2 * 10^{51} erg$
  - 56Ni质量： $M_{56Ni} = 0.11M_{\odot}$ ，完全与抛射物混合
- SN 2017gpn是已确定的距离宿主星系最远的I Ib SN (21 kpc from NGC 1343)

200820

# NGC 2770: high supernova rate due to interaction

<https://arxiv.org/abs/2008.08091>

type:theory-SN

comment:解释NGC 2770的高SN发生率

## ► details

Authors: Michał J. Michałowski, Christina Thöne, Antonio de Ugarte Postigo et al.

Comments: Astronomy & Astrophysics, in press, 8 pages, 3 figures, 1 table

Context. Galaxies that hosted many core-collapse supernova (SN) explosions can be used to study the conditions necessary for the formation of massive stars. NGC 2770 was dubbed an SN factory because it hosted four core-collapse SNe in 20 years (three type Ib and one type IIn). Its star formation rate (SFR) was reported to not be enhanced and, therefore, not compatible with such a high SN rate.

Aims. We aim to explain the high SN rate of NGC 2770.

Methods. We used archival HI line data for NGC 2770 and reinterpreted the H $\alpha$  and optical continuum data.

Results. Even though the continuum-based SFR indicators do not yield high values, the dust-corrected H $\alpha$  luminosity implies a high SFR, consistent with the high SN rate. Such a disparity between the SFR estimators is an indication of recently enhanced starformation activity because the continuum indicators trace long timescales of the order of 100 Myr, unlike the line indicators, which trace timescales of the order of 10 Myr. Hence, the unique feature of NGC 2770 compared to other galaxies is the fact that it was observed very shortly after the enhancement of the SFR. It also has high dust extinction, E(B-V) above 1 mag. We provide support for the hypothesis that the increased SFR in NGC 2770 is due to the interaction with its companion galaxies. We report an HI bridge between NGC 2770 and its closest companion and the existence of a total of four companions within 100 kpc (one identified for the first time). There are no clear HI concentrations close to the positions of SNe in NGC 2770 such as those detected for hosts of gamma-ray bursts (GRBs) and broad-lined SNe type Ic (IcBL). This suggests that the progenitors of type Ib SNe are not born out of recently accreted atomic gas, as was suggested for GRB and IcBL SN progenitors.

- NGC 2770 在20年内发生了4次核塌缩超新星事件（3个Ib 1个IIn），有很高的SN发生率，而其恒星形成率（SFR）没有发现有增大，与高SN发生率不匹配(Thöne et al. 2009)。
- 本篇文章的目标是解释NGC 2770的高SN发生率。
- 分别使用了基于连续谱（continuum-based）和尘埃修正的H $\alpha$ 光度来估算SFR。前者没有给出较高的SFR，后者则给出高的SFR ( $40\text{-}50 M_{\odot}/\text{yr}$ )，与高SN发生率匹配。两种方法的不一致可能是因为前者追踪的时标较长，数量级100Myr；而后者相对较短，为10Myr，表明NGC 2770的恒星形成活动在最近被增强。
- 作者提出NGC 2770 的 SFR 增大的原因是其与伴星系的相互作用。
- NGC 2770 中 SN 发生的位置没有像在GRB和宽线Ic型SN的宿主星系中发现的明显的HI聚集（concentration），表明Ib SN的前身星不像GRB和IcBL SN的前身星那样产生于新近加速吸积的原子气体（recently accreted atomic gas）。

# 200821

---

## The Broad-band Counterpart of the Short GRB 200522A at z=0.5536: A Luminous Kilonova or a Collimated Outflow with a Reverse Shock?

<https://arxiv.org/abs/2008.08593>

type:observation-sGRB

comment:报道了对 $Swift$ 短爆 GRB 200522A的射电余辉和近红外对应体的发现。这颗爆位于一个红移 $z=0.5536$ 的年轻恒星形成星系中心1kpc开外

► details

Authors: W. Fong (Northwestern/CIERA), T. Laskar, J. Rastinejad et al.

Comments: 33 pages, 13 figures, 5 tables. Submitted to AAS Journals

We present the discovery of the radio afterglow and near-infrared (NIR) counterpart of the Swift short GRB 200522A, located at a small projected offset of  $\approx 1$  kpc from the center of a young, star-forming host galaxy at  $z=0.5536$ . The radio and X-ray luminosities of the afterglow are consistent with those of on-axis cosmological short GRBs. The NIR counterpart, revealed by our HST observations at a rest-frame time of  $\approx 2.3$  days, has a luminosity of  $\approx (1.3 - 1.7) \times 10^{42} \text{ erg/s}$ . This is substantially lower than on-axis short GRB afterglow detections, but is a factor of  $\approx 8\text{-}17$  more luminous than the kilonova of GW170817, and significantly more luminous than any kilonova candidate for which comparable observations exist. The combination of the counterpart's color ( $i - y = -0.08 \pm 0.21$ ; rest-frame) and luminosity cannot be explained by standard radioactive heating alone. We present two scenarios to interpret the broad-band behavior of GRB 200522A: a synchrotron forward shock with a luminous kilonova (potentially boosted by magnetar energy deposition), or forward and reverse shocks from a  $\approx 14^\circ$ , relativistic ( $\Gamma_0 \gtrsim 80$ ) jet. Models which include a combination of enhanced radioactive heating rates, low-lanthanide mass fractions, or additional sources of heating from late-time central engine activity may provide viable alternate explanations. If a stable magnetar was indeed produced in GRB 200522A, we predict that late-time radio emission will be detectable starting  $\approx 0.3\text{-}6$  years after the burst for a deposited energy of  $\approx 10^{53}$  erg. Counterparts of similar luminosity to GRB 200522A associated with gravitational wave events will be detectable with current optical searches to  $\approx 250$  Mpc.

- 本文报道了对 $Swift$ 短爆 GRB 200522A的射电余辉和近红外对应体的发现。这颗爆位于一个红移 $z=0.5536$ 的年轻恒星形成星系中心1kpc开外。
- 余辉的射电光度和X射线光度与正轴宇宙学短伽玛爆一致。
- 哈勃拍摄的静系2.3天近红外图像光度为 $\approx (1.3 - 1.7) \times 10^{42} \text{ erg/s}$ , 这显著低于其它正轴短爆的余晖探测, 但比GW170817的kilonova要亮8-17倍。作者估计的  $E_{\gamma,iso}(15 - 150 \text{ keV}) = (8.4 \pm 1.1) \times 10^{49} \text{ erg}$ 。

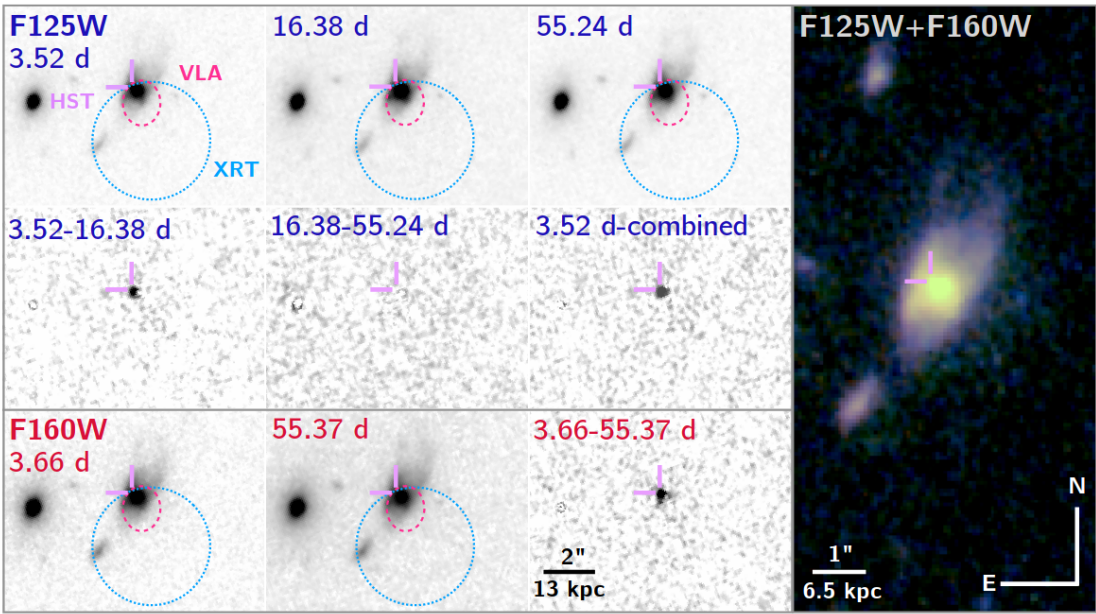


**Figure 2.** *HST/WFC3* observations of GRB 200522A. The three epochs of F125W observations are displayed (top), along with the corresponding HOTPANTS residual images (middle); “combined” refers to a merged template of the F125W observations at 16.38 and 55.24 days. The residual images reveal a fading source between 3.52 and 16.38 days. The two epochs of F160W observations and the subtraction between the two visits are shown in the bottom row. In each of the smaller panels, the XRT position (blue dotted; 90% confidence), VLA position (pink dashed ellipse;  $3\sigma$ ), and *HST* NIR counterpart position (purple cross-hairs) are shown. The scale is denoted in the bottom right panel. The right-hand image is a color composite composed of the merged F125W template and F160W images, with the position of the *HST* counterpart denoted by the purple cross-hairs.

- 该候选体的颜色 ( $i - y = -0.08 \pm 0.21$ ; rest-frame) 以及光度无法仅用标准的放射性加热来解释，作者提出了两种情景解释GRB 200522A的宽频行为：

- 同步辐射的前向激波加上一个较亮的kilonova（可能由磁星的energy deposition驱动）

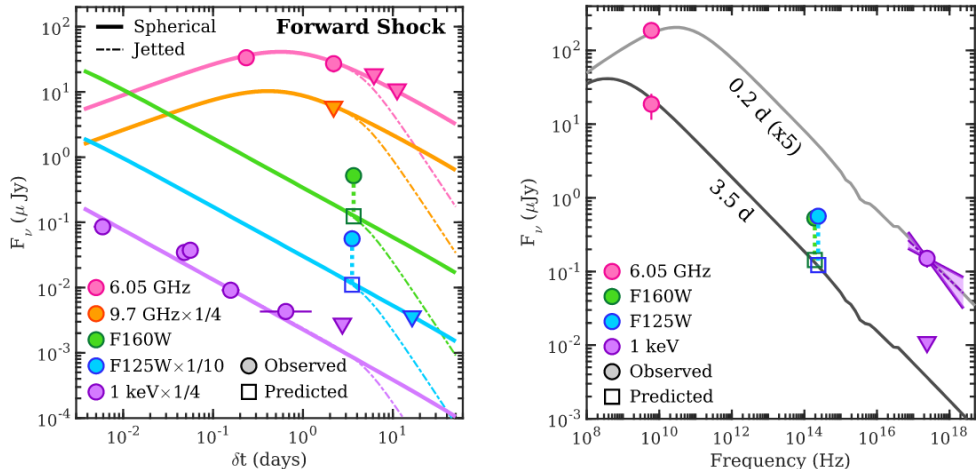


**Figure 4.** The radio, NIR and X-ray observations of the counterpart of GRB 200522A (circular points) and models in Scenario I. *Left:* Representative afterglow model light curves representing a forward shock propagating into the circumburst medium for a spherical outflow (solid lines) and a jetted outflow (dot-dashed lines). If a jet break exists, the observations constrain the time of the break to  $\delta t \gtrsim 3.5$  days. *Right:* The corresponding afterglow model’s spectral energy distributions at  $\delta t = 0.2$  days and 3.5 days; jetted and spherical models are the same at these times. In both panels, models and data points are scaled as denoted for clarity. Error bars correspond to  $1\sigma$  and are generally smaller than the size of the symbols, and triangles correspond to  $3\sigma$  upper limits. The radio and X-ray afterglow temporal and spectral evolution are consistent with the forward shock model, and the measured X-ray spectral slope (purple regions, representing  $1\sigma$  confidence region) is in agreement with the model. Meanwhile, the observed F125W and F160W fluxes at  $\delta t = 3.52$  and 3.66 days are in excess of the predicted fluxes (open squares) by factors of  $\approx 5 - 10$ .

- 14度角的相对论性 ( $\Gamma_0 \gtrsim 80$ ) 喷流中的前向和反向激波

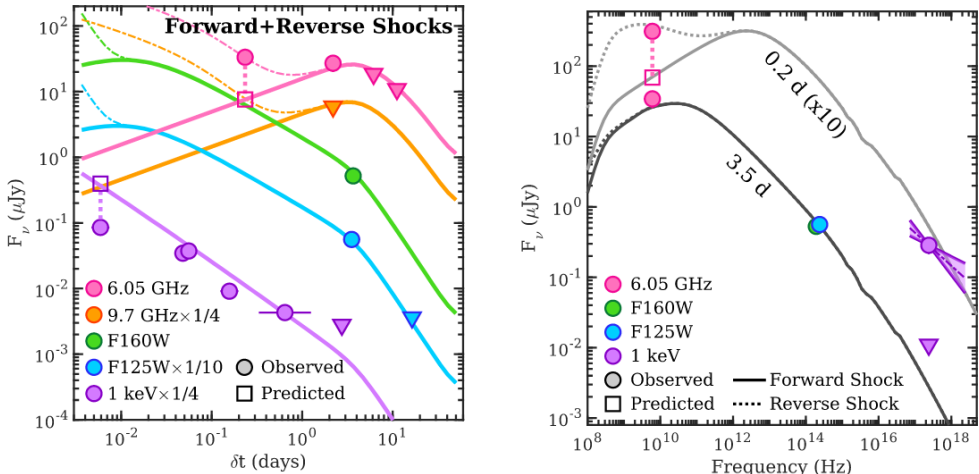


**Figure 6.** The radio, NIR and X-ray observations of the counterpart of GRB 200522A (circular points) and models in Scenario II. *Left:* Representative afterglow model light curves representing a forward shock with an achromatic jet break at  $t_{\text{jet}} = 4.0$  days (solid lines). The radio data point at  $\delta t \approx 0.23$  days is in excess of the model, and can be explained by the addition of a reverse shock (dot-dashed lines). *Right:* The corresponding afterglow model spectral energy distributions at  $\delta t = 0.2$  days and 3.5 days, including forward shock only (solid lines) and forward and reverse shocks (dot-dashed lines). In this scenario, the NIR-band temporal evolution is consistent with the forward shock model with a jet break, but is steeper than the observed X-rays, and under-predicts the early radio emission. In addition, the measured X-ray spectral slope (purple regions, representing  $1\sigma$  confidence region) is shallower than the predicted slope of  $\beta_X = -1$ . In both panels, models and data points are scaled as denoted for clarity. Error bars correspond to  $1\sigma$  and are generally smaller than the size of the symbols, and triangles correspond to  $3\sigma$  upper limits.

- PS1  $y : \lambda_{\text{eff}} = 9613.5$
- 另外包括增强的放射性加热率、低镧系元素质量、或来自晚期中心引擎活动的额外加热源都可能提供可行的解释。
- 如果GRB 200522A 中产生了稳定磁星，作者预测，对于deposited energy of  $\approx 10^{53}$  erg，将在爆后约0.3-6年开始探测到晚期射电辐射。

**PAN-STARRS filters:**

Filter ID	$\lambda_{\text{mean}}$	$\lambda_{\text{eff}}$	$\lambda_{\text{min}}$	$\lambda_{\text{max}}$	$W_{\text{eff}}$	ZP (Jy)	Obs. Facility	Instrument	Description
PAN-STARRS/PS1.g	4900.1	4810.9	3943	5593	1053.1	3893.0	PAN-STARRS	PAN-STARRS	PS1 g filter
PAN-STARRS/PS1.r	6241.3	6156.4	5386	7036	1252.4	3135.5	PAN-STARRS	PAN-STARRS	PS1 r filter
PAN-STARRS/PS1.w	6579.2	5985.9	3966	8344	2561.7	2937.2	PAN-STARRS	PAN-STARRS	PS1 w filter
PAN-STARRS/PS1.open	7461.4	6439.4	3800	10755	3985.0	2603.0	PAN-STARRS	PAN-STARRS	PS1 open filter
PAN-STARRS/PS1.i	7563.8	7503.7	6778	8304	1206.6	2577.0	PAN-STARRS	PAN-STARRS	PS1 i filter
PAN-STARRS/PS1.z	8690.1	8668.6	8028	9346	997.7	2273.0	PAN-STARRS	PAN-STARRS	PS1 z filter
PAN-STARRS/PS1.y	9644.6	9613.5	9100	10838	639.0	2203.7	PAN-STARRS	PAN-STARRS	PS1 y filter

## Pre-supernova evolution, compact object masses and explosion properties of stripped binary stars

<https://arxiv.org/abs/2008.08599>

type:theory-pre\_SN\_star

comment:单星和包层剥离的双星之间在爆发SN之前的结构存在系统性差异(关键的量是CO核心质量和氢燃烧后炭的丰富度)，因此导致SN的不同

► details

Authors: F.R.N. Schneider, Ph. Podsiadlowski, and B. Müller

Comments: 24 pages (incl. appendix), 17 figures, 2 tables; submitted to A&A; comments welcome

The era of large transient surveys, gravitational-wave observatories and multi-messenger astronomy has opened up new possibilities for our understanding of the evolution and final fate of massive stars. Most massive stars are born in binary or higher-order multiple systems and exchange mass with a companion star during their lives. In particular, the progenitors of a large fraction of compact object mergers, and Galactic neutron stars (NSs) and black holes (BHs) have been stripped off their envelopes by a binary companion. Here, we study the evolution of single and stripped binary stars up to core collapse with the stellar evolution code Mesa and their final fates with a parametric supernova (SN) model. We find that stripped binary stars can have systematically different pre-SN structures compared to genuine single stars and thus also different SN outcomes. The bases of these differences are already established by the end of core helium burning and are preserved up to core collapse. Consequently, we find that Case A & B stripped stars and single & Case C stripped stars develop qualitatively similar pre-SN core structures. We find a non-monotonic pattern of NS and BH formation as a function of CO core mass that is different in single and stripped binary stars. In terms of initial masses, single stars of 35  $M_{\odot}$  all form BHs, while this transition is only at about 70  $M_{\odot}$  in stripped stars. On average, stripped stars give rise to lower NS and BH masses, higher explosion energies, higher kick velocities and higher nickel yields. Within a simplified population synthesis model, we show that our results lead to a significant reduction of the rates of BH-NS and BH-BH mergers with respect to typical assumptions made on NS and BH formation. Therefore, we predict lower detection rates of such merger events by, e.g., advanced LIGO than is often considered. We further show how certain features in the NS-BH mass distribution of single and stripped stars relate to the chirp-mass distribution of compact object mergers. Further implications of our findings are discussed with respect to the missing red-supergiant problem, a possible mass gap between NSs and BHs, X-ray binaries and observationally inferred nickel masses from Type Ib/c and IIP SNe.

- 单星和包层剥离的双星之间在爆发SN之前的结构存在系统性差异(关键的量是CO核心质量和氢燃烧后碳的丰富度), 因此导致SN的不同。这些差异在核心氦燃烧结束时已经开始存在, 一直延续到核塌缩。
- 初始质量大于35倍太阳质量的单星最后都会形成黑洞, 而对于剥离双星, 这个质量是70太阳质量。
- 平均而言, 剥离恒星会导致较低的NS和BH质量, 较高的爆炸能量, 较高的反冲速度和较高的Ni产率。
- 简化的population综合模型表明, 本文的结果将导致BH-NS和BH-BH并合的几率将会比传统预期大大降低。